



An advanced perception model combining brain noise and adaptation

Parth Chholak · Alexander E. Hramov · Alexander N. Pisarchik

Received: 10 January 2020 / Accepted: 4 June 2020
© Springer Nature B.V. 2020

Abstract We develop an advanced model of bistable perception based on the interplay of noise and adaptation. The model describes the decision-making process in the brain consisting in involuntary switches between perceptual states. We study the effects of noise and the stimulus duty cycle on the dominance of a particular externally biased perceptual state. We discuss the biological relevance of our model and compare the obtained numerical results with neurophysiological experiments on brain dynamics. The model qualitatively describes the results of neurophysiological experiments on human perception using bistable images, such as gamma distribution of average dominance times and the effect of brain noise on sustained attention.

Keywords Adaptation · Bistable perception · Brain noise · Perception · Bistability

1 Introduction

The thinking process in the brain, as a multistable dynamical system, can be considered as alternative switching between coexisting mental states [23]. These switches can be either spontaneous or initiated by external stimulation, but in both cases they are triggered by neuronal brain noise. Inherent brain noise was experimentally detected in rat neocortical pyramidal neurons as $1/f$ noise (or pink noise) in membrane potential fluctuations [22]. This kind of noise is common in biological systems, including human cognition [14]. Hausdorff & Peng [16] suggested that a possible source of $1/f$ noise results from different time scales of biological processes. Recently, endogenous brain noise was estimated in neurophysiological experiments using electroencephalography (EEG) [45] and magnetoencephalography (MEG) [41] in subjects observing ambiguous images. A particular case of perceptual bistability with two interpretations of an ambiguous visual stimulus was widely studied in experiments based on binocular rivalry and ambiguity in geometry, figure-ground, and motion direction (for comprehensive review see [1, 30, 33]). Inherent brain noise is known to induce switches between coexisting perceptual states during prolonged gazing of a multistable image [4].

Let us consider, for instance, a bistable image, such as the Necker cube, which can be interpreted as either left- or right-oriented. Viewing this figure for a

P. Chholak (✉) · A. N. Pisarchik
Center for Biomedical Technology, Technical University of Madrid, Campus Montegancedo, 28223 Pozuelo de Alarcón, Spain
e-mail: parth.chholak@ctb.upm.es

A. N. Pisarchik
e-mail: alexander.pisarchik@ctb.upm.es

A. E. Hramov · A. N. Pisarchik
Center for Technologies in Robotics and Mechatronics Component, Innopolis University, 1 Universitetskaya Str., Innopolis, The Republic of Tatarstan, Russia 420500

prolonged time a spontaneous alternation between the two percepts takes place, changing as often as every few seconds [43] and vary among subjects [6]. This alternation has been attributed to neural adaptation or satiation [17, 24]. Random switches between the two percepts were also found in neurophysiological experiments, where the underlying electrical membrane potential was measured [5]. Although these switches are known to be induced by inherent brain noise, the exact microscopic mechanism of these oscillations remains unknown [48].

Noise is ubiquitous in the brain at multiple scales, from vesicular release and spiking variability to fluctuations in a global neurotransmitter level. The sources of endogenous brain noise lie in quasi-random release of neurotransmitters by synapses, random synaptic input from other neurons, random switching of ion channels, stochasticity in N-methyl-D-aspartate activated receptors which affect the stability of short-term memory and attention, random alteration of gamma-amino-butyric acid receptor which activates synaptic ion channel conductances and determine how likely the system jumps into a pathological state [8]. To describe the random cognition process, several formal models based on competition and self-inhibition of representative neuronal populations or engrams (hypothetical traces in the memory that represent each object) were suggested [27, 28, 52]. In these models, the competition is manifested between the competing perceptual neuronal populations by means of the reciprocal inhibition accompanied by a slow adaptation of the dominant population [21]. To date, the presence of noise and adaptation in neural perception is accepted by many researchers and widely reported in scientific literature (see, e.g., [3, 10, 37, 39, 47]). In particular, Huguet et al. [21] suggest that adaptation plays an important role in determining perceptual choice, while brain noise induces randomness in switching over different engrams [49]. In the oscillatory models, the switching is primarily driven by adaptation, while in the noise-driven energy models, noise is the only reason behind switches between coexisting attractors. The main drawback of the latter models is that they are not able to simulate such experimental data as resting time histogram shapes and correlations between durations of successive engrams. Instead, the combination of both models would allow gauging relative strengths of noise and adaptation. Therefore, empirically obtained

arbitrary parameters, such as a stimulus amplitude, noise intensity, and strengths of mutual inhibition and adaptation are meaningful in relation to each other, and the qualitative behavior of perception in the model context should in turn portray a real cognitive process.

The aim of this work is to capture the essence of adaptation processes in a simplistic mechanism of bistable perception assisted by brain noise with minimal elements and assumptions. The model is inspired from the motion quartet model of Hock et al. [19] with four competing neurons, each dependent on its own abstract adaptation variable. The results of the recent MEG experiments [41] closely match the model prediction in the metastable regime.

2 Model

It can be argued that there are no object-specific neurons (or engrams) inside the brain [44], there rather exists a feature-specific neuronal network with a finite number of neurons which can be suitably co-activated to form a unique representation of each object or thought [50]. However, the neuronal clusters representing each feature may internally compete to manifest the degree to which the feature sub-population as a whole is excited. This means that the same ambiguous image can excite or inhibit different sets of neurons depending on its interpretation.

In the case of bistable perception, let us to denote two extreme perceptions or states as X and Y . Since the same stimulus causes both perceptions, the feature space remains the same for both and hence, all excited or inhibited neurons (feature-specific) for both perceptions are common. Examples of such feature-specific neurons are neurons dedicated to capturing basic colors, length, width, depth, motion direction [51], and orientation.

Let the total number of such feature-specific neuronal clusters be N . Hereinafter, for simplicity we refer to these clusters as *single neurons*. However, the reader can understand them as a co-activated cluster of neurons reflecting a sensory input feature. Now, imagine a N -dimensional feature space representing the activation (membrane potential or spiking rate) for each of the N neurons. In this space, X and Y are two separate points. Many neurophysiological experiments are devoted to the study of the perception transition based on the variation of a single feature-

space parameter biasing one perception over the other, while keeping all other features the same. To fit the scope of these experiments, we simplify our model by fixing the stimulus in $(N - 1)$ dimensions and varying it only in one dimension. So, the primary dynamics can be seen in that dimension and the rest of the space can be kept aside for simplicity. Hence, we will treat X as a scalar and not as a vector with N components. In the future work, we may generalize the model to include a more diverse feature set within the same framework only by increasing the dimensional space in which we define X .

Our sensory organs undergo random fluctuations of physiological variables (endogenous noise), such as body temperature, blood pressure, spontaneous neuronal activity, that result in physiological tremor. However, we do not feel these fluctuations, so our perception remains quite stable. Therefore, the above consideration requires us to introduce a *self-stabilization* mechanism into the perception model.

Numerous empirical studies of bistable perception, as well as discussions with other researchers suggest that at every moment of time, a person is capable to interpret an ambiguous stimulus in only one of the possible ways, and never make two or more decisions simultaneously. In this regard, the brain works similar to a computer, but with a much slower clock rate. The volume of information we receive each day is enormous, and a large part of this information is ignored by the brain. This way, we only focus on the most important details, which form a very small segment of the environment. This means that a decision-making process in favour of one of the possible solutions suppresses all other solutions. Therefore, in our model, we also need to introduce a term that captures *competitive inhibition* between coexisting states. Taking into account the nature of the synaptic input processing, which implies the neuron firing only if the input signal is sufficiently strong (otherwise, the neuron is silent), we use a sigmoidal function to model synaptic connections for competitive inhibition, as follows

$$\sigma(X) = \frac{1}{1 + e^{-\beta X}} \tag{1}$$

Next, our model needs to capture adaptation which reveals itself as a slow self-destabilization tendency to any stimulus interpretation. When we receive an ambiguous stimulus and fix our attention on one of the

possible interpretations, after a certain period of time our attention involuntarily switches to another interpretation. These switches are irregular due to endogenous brain noise. However, the mean duration of each percept, measured in psychological experiments on bistable visual perception, is rather regular [31, 38]. This suggests that apart from brain noise there also exists a deterministic mechanism referred to as *adaptation*, which induces involuntary transitions between perceptual states.

To account for adaptation in our model, we introduce a variable representing each percept in the working memory [13, 46], which tracks the activity of the percept. If the activity is prolonged enough, then adaptation destabilizes the active neuronal state. For this reason, the time constant for the memory state should be much larger than that for the perceptual states. This is congruent with our idea of the brain ability to maintain only a stable perception in memory, that must not concur with random fluctuations in perception. Only after the stimulus is clearly perceived, it begins to register in the memory. For this reason, we again use the sigmoidal function for perception states (say X and Y) to affect memory states (X_m and Y_m). We assume that the memory states are also self-stabilized to ensure that spontaneous switching does not occur in the memory until the specific causal perception of this memory has changes. Moreover, memory activation should be significantly stronger than random fluctuations in order to destabilize current perception through adaptation. Hence, we will again use the sigmoidal function to capture the

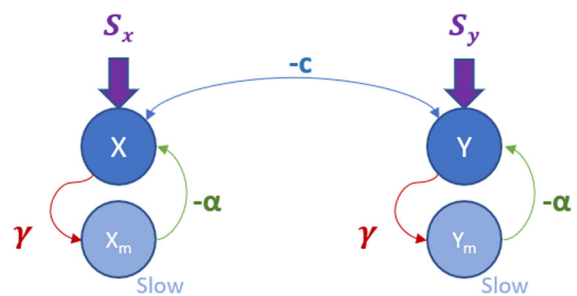


Fig. 1 Schematic illustration of the advanced perception adaptation model. X_m and Y_m are memory neuron states inhibitory coupled with perceptual states X and Y , which in turn are inhibitory coupled with each other, α and γ are the corresponding coupling strengths, and h and h_m are the resting potential for perceptual states and working memory, respectively. The big arrows indicate the inputs of stimuli S_x and S_y

memory effect on the perceptual state. A schematic representation of our model is illustrated in Fig. 1.

Keeping in mind the above consideration, the perception model can be introduced as follows:

$$\tau \dot{X} = S_X + h - X - c\sigma(Y) - \alpha\sigma(X_m) + \eta \xi_X(t), \tag{2a}$$

$$\tau_m \dot{X}_m = h_m - X_m + \gamma\sigma(X) + \eta_m \xi_{X_m}(t), \tag{2b}$$

$$\tau \dot{Y} = S_Y + h - Y - c\sigma(X) - \alpha\sigma(Y_m) + \eta \xi_Y(t), \tag{2c}$$

$$\tau_m \dot{Y}_m = h_m - Y_m + \gamma\sigma(Y) + \eta_m \xi_{Y_m}(t), \tag{2d}$$

where X and Y are perceptual neuronal states, X_m and Y_m are memory states, S_X and S_Y are input signals, α is a coefficient associated with the strength of adaptation, and c is a constant representing the strength of suppression by the winner state on the losing state or competitiveness coefficient. The competitiveness coefficients for both perceptual states are taken to be the same because any state can win the competition initially and suppress the loser neuron with equal strength. The ratio between S_X and S_Y is determined by the stimulus ambiguity. When the stimulus is completely ambiguous (as, e.g., a bistable Necker cube), we deal with an unbiased signal, i.e. $S_X = S_Y$.

To account for endogenous brain noise, independent zero-mean Gaussian noise ξ of intensities η and $\eta_m = \sqrt{\tau/\tau_m}\eta$ is added in Eq. (2) to perception and memory variables, respectively. This noise is generated using an in-built function of MATLAB (*randn*) for producing normally distributed random numbers. The probability density function of a random variable z is given by

$$p(z) = \frac{1}{\sigma\sqrt{2\pi}} \exp\left[-\frac{(z-\mu)^2}{2\sigma^2}\right],$$

where $\mu = 0$ is mean and $\sigma = 1$ is standard deviation. For the perceptual (X and Y) and memory (X_m and Y_m) neurons, τ and τ_m are time constants, and h and h_m are resting potentials in the absence of any stimulus. Since the same set of perceptual neurons is involved in the processing of both input signals, the time constant is kept the same for both states. For the memory neurons, γ is a coefficient which determines how much the choice of the current state affects the memory.

The parameter values are present in Table 1. The choice of parameters is directly linked to the motion quartet model of Hock et al. [19], where exactly the same values were used for parameters τ , τ_m , h , h_m , α , γ , and η . The resting potentials h and h_m are chosen negative, so that they cannot have a suppressing effect on the active neuronal population, as the sigmoidal function decays to zero for negative input values. Next, the amplitude of stimulating signals in their model was varied between 12 and 20. Due to the reduction in the number of participating neurons, we choose $|S_X| = |S_Y| = 10$. The cross-coupling between the four neurons in their model was heterogeneous and took values of either 3.5 or 7. In our model we choose a similar value of $C = 5$. In addition, we take $\beta = 5$ to ensure a sufficiently nonlinear behavior of the σ -function for synaptic connectivity. Lastly, we vary duty cycle d from 0 to 1 to cover all extremes, from no stimulation to uniform stimulation, as well as other periodic stimulation variants in between.

3 Analytical study of the deterministic system

The analytical study is performed for the deterministic case, i.e., for $\eta = \eta_m = 0$ in Eqs. (2a)–(2d).

3.1 Linear approximation

For the explored set of the parameters (see Table 1), the exact solution of the system cannot be found analytically. In order to find an equilibrium point, we approximate the sigmoidal function in Eq. 1 by the linear slope

$$\sigma(X) \sim \frac{5}{4} \left(X + \frac{2}{5} \right), \tag{3}$$

tangent to it at $X = 0$, as shown in Fig. 2.

For the same input signal to both perceptual neurons X and Y , the system in Eq. (2) is symmetric and hence we expect symmetric steady states. Using this observation to simplify calculations, the fixed-point analysis yielded the equilibrium point

$$(X, Y, X_m, Y_m) = (0, 0, 0, 0).$$

The linear stability analysis at this point shows that the largest real part of eigenvalues $\Re(\lambda)_{\max} = 0.2467$ is positive, i.e., the fixed point is unstable for the set of

Table 1 Parameter values

| Parameter | τ | τ_m | h | h_m | S_X | S_Y | c | α | β | γ | η | d |
|-----------|--------|----------|-----|-------|-------|-------|-----|----------|---------|----------|--------|-------|
| Value | 20 | 1000 | -5 | -5 | 10 | 10 | 5 | 5 | 5 | 10 | 0 - 1 | 0 - 1 |

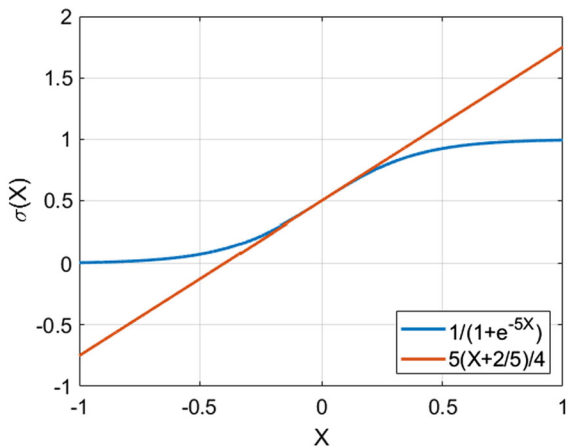


Fig. 2 Linear approximation of the sigmoidal function in Eq. 1 for $\beta = 5$

the system parameters given in Table 1. The stability of the fixed point depends on the system parameters.

In Fig. 3, we show how the largest real part of eigenvalues of the fixed point depends on the suppression strength c and time scales ratio τ_m/τ . One can see from Fig. 3a that the fixed point is stable ($\Re(\lambda)_{\max} < 0$) only for small c and small ratios

between the time scales of memory and perception (τ_m/τ). For other fixed parameters (see Table 1), the fixed point is only stable for $\tau_m/\tau < 0.2$, as seen from Fig. 3b. Thus, the high difference between the time scales of memory τ_m and perception (τ) is crucial for the fixed point stability. Since memory is always much longer than the perception time ($\tau_m \gg \tau$), the fixed point is always unstable.

On the other hand, the perceptual neurons in our model should be responsive for activation, while the memory neurons for inhibition. In order to avoid the inhibition which perpetually suppresses any neural activity, we need to keep the activity of the memory neurons slower than that of the perceptual neurons.

3.2 Fixed point analysis in the absence of memory adaptation

Let us now consider an alternate scenario which would happen in the absence of memory adaptation ($\alpha = 0$). In this case, we deal with a unidirectional coupling between the respective activation and memory. Therefore, we first solve the equations for X and Y variables,

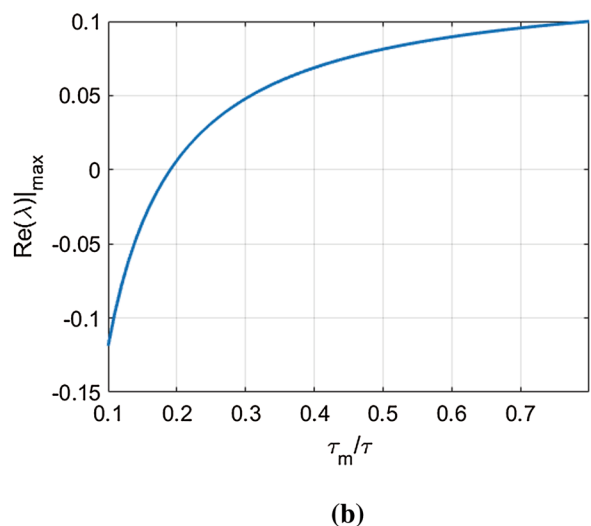
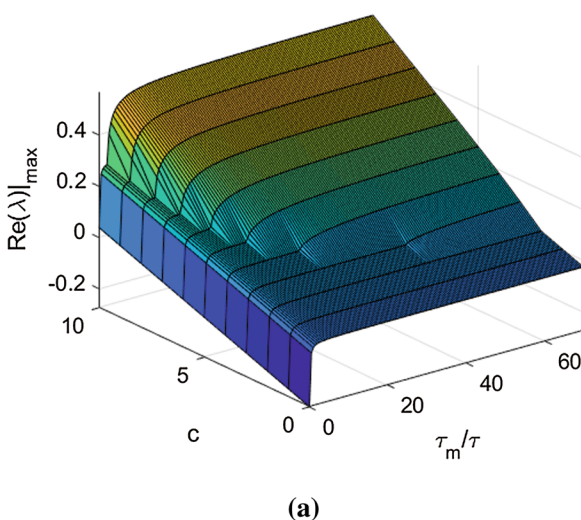


Fig. 3 The largest real part of eigenvalues versus competitiveness (c) and ratio (τ_m/τ) between time scales of memory and perception

and then evaluate X_m and Y_m which depend on the steady-state values of the former variables.

Taking $\alpha = 0$, $\eta = 0$ and keeping all other parameters as in Table 1, we equate Eq. (2) to zero to calculate fixed points. As a result, we get

$$X = 5 - 5\sigma(Y), \tag{4a}$$

$$X_m = -5 + 10\sigma(X), \tag{4b}$$

$$Y = 5 - 5\sigma(X), \tag{4c}$$

$$Y_m = -5 + 10\sigma(Y). \tag{4d}$$

As seen from Fig. 2, the range of σ -function is from 0 to 1 with $\sigma(0) = 0.5$. Simple computations show that Eqs. (4a) and (4c) would iteratively converge to either $(X, Y) = (0, 2.5)$ or $(X, Y) = (2.5, 0)$. The calculations of $(X_m, Y_m) = (0, 5)$ and $(X_m, Y_m) = (5, 0)$ are straightforward from Eqs. (4b) and (4d). Thus, in the absence of memory adaptation, there are two possible fixed point solutions (FP_1 and FP_2):

$$(X, Y, X_m, Y_m)^{FP_1} = (0, 2.5, 0, 5),$$

$$(X, Y, X_m, Y_m)^{FP_2} = (2.5, 0, 5, 0).$$

The obtained results are reminiscent of the winner-takes-all behavior of the activation variables X and Y . Here, the steady-state solution depends on initial conditions only.

3.3 Reduced dynamical equations

Owing to the symmetry between X and Y variables and their reciprocative behaviors, we may opt for an even more sophisticated approach for analytical analysis of the system to shed light on some of the key features of the system. The results of our numerical simulations presented below (Fig. 4a) demonstrate that the variables X and Y oscillate in antiphase. Using this property and after substituting the parameter values given in Table 1 for zero noise ($\eta = 0$) into Eqs. (2a) and (2b), they can be rewritten as

$$20\dot{X} = -X + 5 - 5\sigma(-X) - 5\sigma(X_m), \tag{5a}$$

$$1000\dot{X}_m = -X_m - 5 + 10\sigma(X). \tag{5b}$$

Next, multiplying Eq. (5a) by (-2) and adding to Eq. (5b), we get

$$1000\dot{X}_m - 40\dot{X} = 2X - X_m - 15 + 10\sigma(X_m) + 10[\sigma(X) + \sigma(-X)]. \tag{6}$$

A simple calculation gives

$$\sigma(X) + \sigma(-X) = \frac{1}{1 + e^{-\beta X}} + \frac{1}{1 + e^{\beta X}} = 1. \tag{7}$$

Therefore, using Eq. (7), we can simplify Eq. (6) into

$$1000\dot{X}_m - 40\dot{X} = 2X - X_m - 5 + 10\sigma(X_m). \tag{8}$$

From Fig. 4a, one can see that X and Y vary approximately between -4 and $+4$, while X_m and Y_m between -0.5 and $+0.5$. At the same time, the linear approximation of the sigmoidal function in the $[-0.5, 0.5]$ range is not far from reality (see Fig. 2), whereas the linear approximation for X and Y variables outside this domain would be grossly incorrect. The steps from Eq. (5) to Eq. (8) have been directed to get a rid of the dependence on $\sigma(X)$, and hence we will only use the linear approximation for $\sigma(X_m)$ in the justified $[-0.5, 0.5]$ domain. Therefore, using the linear approximation stated in Eq. (3), we can rewrite Eq. (8) as

$$1000\dot{X}_m - \frac{25}{2}X_m = 2X + 40\dot{X}. \tag{9}$$

One of possible solutions of the simplified Eq. (9) may be a harmonic signal $X = A \cos(\omega t)$, whose amplitude A and frequency ω are chosen from numerical simulations (as in Fig. 4a) to obtain similar dynamics, specifically, $A = 4$ and the modulation period $T = 4500$. Substituting the cosine function in Eq. (9), we get

$$1000\dot{X}_m - \frac{25}{2}X_m = 8 \cos(\omega t) - 160\omega \sin(\omega t), \tag{10}$$

where

$$\omega = \frac{2\pi}{4500} \approx 1.40 \times 10^{-3}.$$

Equation (10) can be simplified to

$$\dot{X}_m + kX_m = B \cos(\omega t + \theta), \tag{11}$$

where $k = -25/2000$, $\theta = 0.03$, $B = 8/1000$, θ is the initial phase difference. Ignoring the initial phase difference ($\theta = 0$), that only shifts the input signal

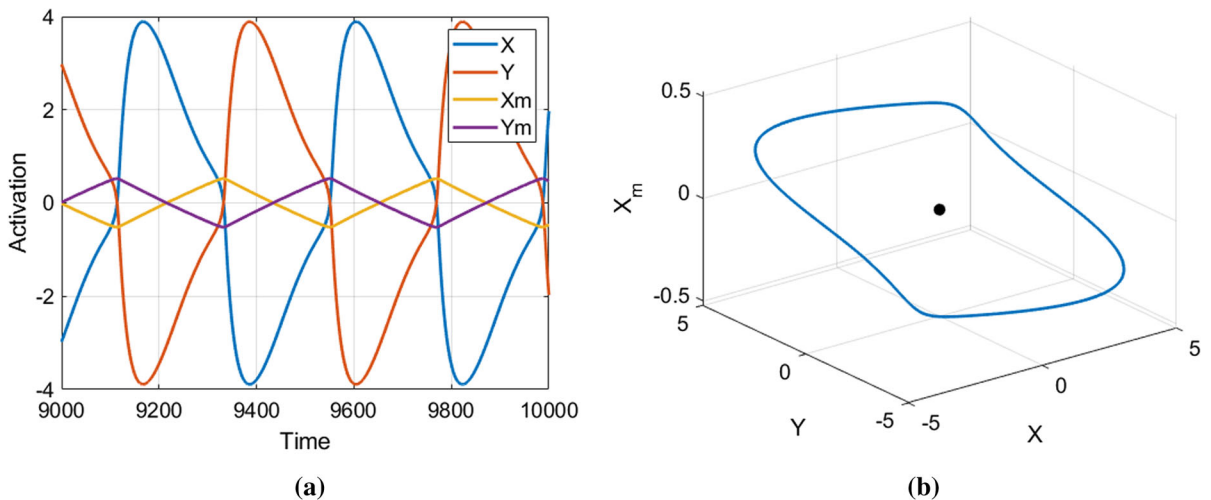


Fig. 4 Deterministic dynamics ($\eta = 0$) of Eq. (2) illustrated with **a** time series and **b** phase portrait. The dot in the phase portrait indicates the location of the unstable fixed point found analytically in Sect. 3.

marginally to the right on the time-axis, we look for X_m in the following form

$$X_m(t) = C \cos(\omega t - \phi), \tag{12}$$

where $C = B/\sqrt{K^2 + \omega^2} = 0.64$ and $\phi = \tan^{-1}(\omega/K) = -0.11$.

This analytical solution matches the results of the numerical simulations (Fig. 4a) in the following aspects:

- (i) X_m exhibits a periodic behavior with an amplitude close to 0.5.
- (ii) The modulation frequency is the same.
- (iii) X_m lags behind X .

A better analytical solution might be revealed using a closer approximation of the numerically found X function presented in Fig. 4a. An alternate approach to solve Eq. (9) could be applied if instead of X we approximate X_m by a triangle function, since the numerically calculated X_m variable has a triangular shape. However, a triangular wave is not smooth and therefore not differentiable, that creates additional difficulty.

4 Numerical simulations

In order to find numerical solutions of Eq. (2), we carry out numerical simulations using the Euler-Maruyama scheme.

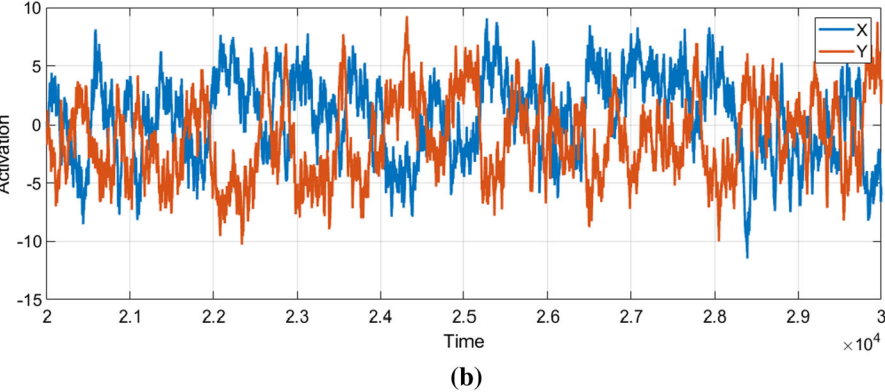
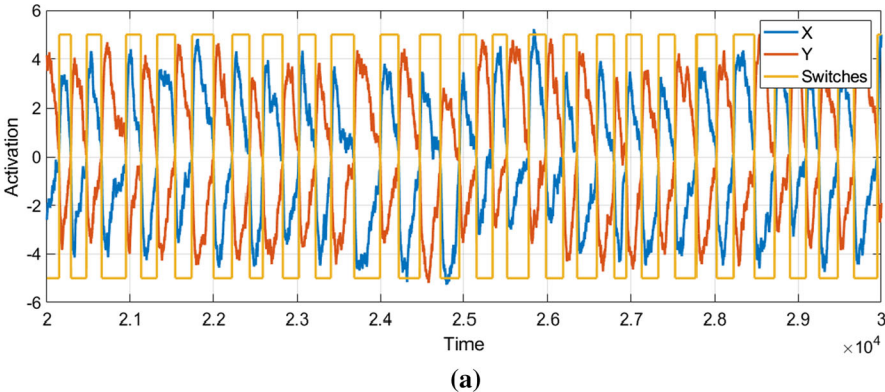
4.1 Deterministic case

First, we simulate deterministic dynamics ($\eta = 0$) of Eq. (2) with uniform and unbiased stimulation ($S_X = S_Y = 10$). The time series and the corresponding phase portrait are present in Fig. 4a, b, respectively. From the time series, one can see that the variables X and Y , as well as the variables X_m and Y_m , periodically alternate with each other representing a stable limit cycle shown in Fig. 4b.

4.2 Stochastic case

The application of additive noise destabilizes the limit cycle resulting in stochastic oscillations, as shown in Fig. 5. As discussed in Sect. 1, the duration of the activation of each state is a random variable with a characteristic time of few seconds, due to the adaptation mechanism described above. This means that each switch occurs after a certain random time interval. Following Hock et al. [19], in our model, we use Gaussian noise due to its popularity in natural systems and easy implementation. We have also found in our recent experimental MEG study on visual perception of flickering images [41] that brain noise in some subjects displayed Gaussian probability distribution, whose kurtosis was close to 3. Nevertheless, in future works, it would also be informative to model noise using non-Gaussian noise [9] to check whether it improves the results and predictions of our model.

Fig. 5 Time series of the stochastic system in Eqs. (2) with noise intensities **a** $\eta = 0.1$ and **b** $\eta = 0.5$. The square yellow line shows switches recognized with the 3η -criterion



Essentially, noise-induced drifts in the activation variable trajectory affect the relative values of X and Y , which in turn determine the amount of competitive inhibition between the two perceptual states. This leads to early or late switches between the perceptual states, deterministically induced by adaptation. One can see that now the trajectory randomly alternates between two perceptual states. The switches can be recognized using different criteria. For definiteness, we choose a 3η criterion since it yields the best statistical results. This criterion states that a switch is recognized when the difference between X and Y variables crosses the threshold value defined as $|X - Y| = 3\eta$, as illustrated in Fig. 5a.

In order to characterize stochastic dynamics, we calculate the number of switches between X and Y perceptual states as a function of the noise intensity. As seen from Fig. 6, for relatively strong noise ($\eta > 0.3$), the number of switches grows linearly as the noise intensity is increased.

Next, we are also interested in how noise affects the dominance duration, i.e., the time the system spends in the perceptual states. Given that we now know about

time instants corresponding to switches in perception using the 3η -criterion discussed above, the intervals between these switches indicate the time the system spends in each perceptual state. When the dominance intervals in Fig. 5a occur in the positive region, the X -state is dominant, whereas the negative region

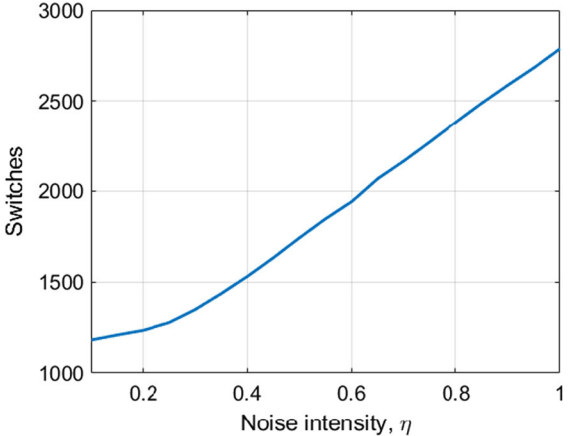


Fig. 6 Number of switches versus noise intensity during $t = 2.5 \times 10^5$

indicates the Y -state dominance. In Fig. 7 we plot the probability distributions of the dominance durations for three different intensities of noise. While for weak noise the distribution is somewhat Gaussian (Fig. 7a), for intermediate values of the noise intensity it is close to a gamma distribution (Fig. 7b) typical for biological systems [29, 38], whereas for very strong noise, the distribution is exponential (Fig. 7c).

The simulations also show that the most probable (mode) dominance duration decreases as the noise intensity is increased (Fig. 8). This result is in a good agreement with experiments on bistable perception [7, 38, 43].

Stochastic dynamics can also be characterized by coherence as a measure of order [2, 12, 42], that can be calculated in terms of correlation time τ_c as [40]

$$\tau_c = \int_0^\infty C^2(t)dt, \tag{13}$$

where C is the normalized autocorrelation function given as

$$C(\tau) = \frac{\langle (X(t) - \langle X(t) \rangle)(X(t + \tau) - \langle X(t) \rangle) \rangle}{\langle (X(t) - \langle X(t) \rangle)^2 \rangle}, \tag{14}$$

where $\langle \dots \rangle$ means averaging and τ is the lag time. The larger the correlation time τ_c , the higher the coherence.

As seen from Fig. 9, the dependence of the correlation time on the noise intensity can be approximated by the power law $\tau_c \sim e^{-0.73}$ with the characteristic exponent close to $-3/4$.

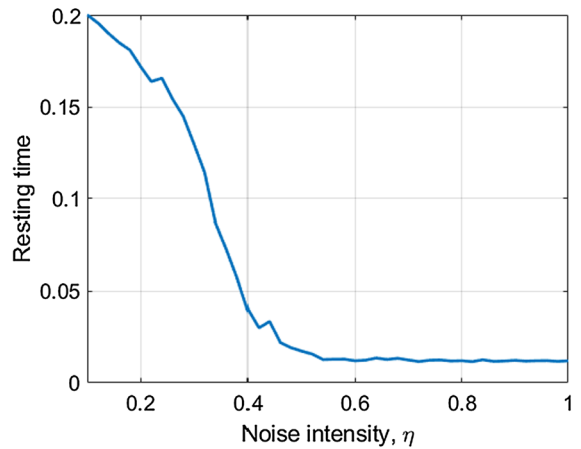


Fig. 8 Mode dominance duration versus noise intensity

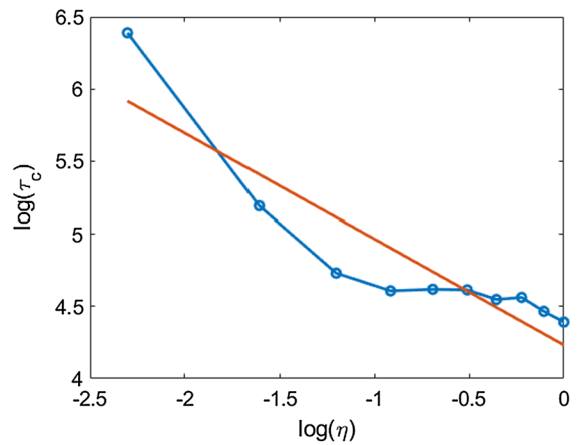


Fig. 9 Correlation time versus noise intensity. The straight red line is a power-law approximation which yields a -0.73 slope

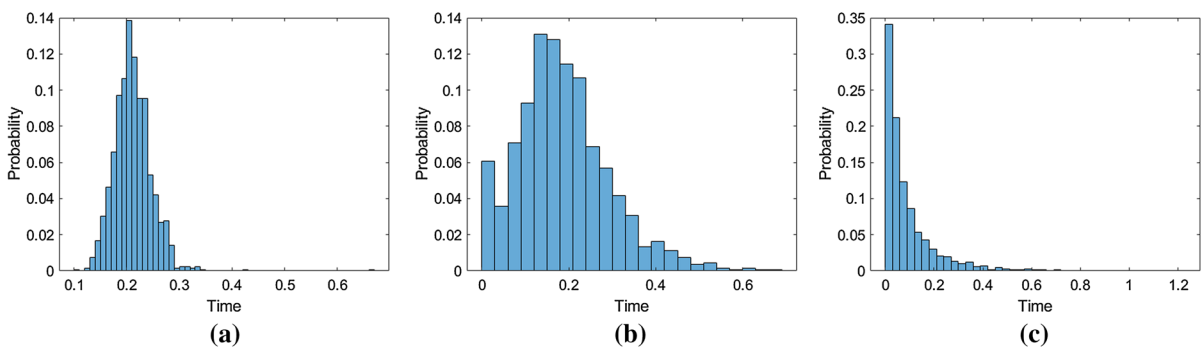


Fig. 7 Probability distributions of dominance durations for noise intensities **a** $\eta = 0.1$, **b** $\eta = 0.3$, and **c** $\eta = 1$

4.3 Habituation

In their paper, Leopold et al. [31] reported that the perceptual alternation may be slowed down, and even brought to a standstill, if a visual stimulus is periodically removed from view. To simulate such a behavior, we apply a square-shape modulation to both stimuli S_X and S_Y as follows

$$S_X = |S_X| \text{ square } (t), \tag{15a}$$

$$S_Y = |S_Y| \text{ square } (t), \tag{15b}$$

where $|S_Y| = 10$ and $|S_X| = \{8, 9, 10, 11, 12\}$ are the stimulus amplitudes such that the stimulus signals go from 0 to $|S_X|$ or to $|S_Y|$.

The results of the periodic neuron activation with period $p = 50$ are present in Fig. 10. One can see that during a prolonged time ($t \approx 1500$), the Y state remains excited, while the X is inhibited. Then, the system dynamics changes so that the inhibited state becomes excited. If we compare this figure with Fig. 5a, we can see that the dominance time for one of the states enlarges in the presence of modulation (1500 versus 400). This means that the periodic modulation stabilizes the perceptual states. The stabilization effect was highlighted in many neurophysiological experiments with bistable perception [20, 25, 34, 35].

One can see from Fig. 10 that the memory state variable Y_m gradually increases from a negative value to a value close to zero; this causes the state Y inhibition and the X state excitation.

4.3.1 Effect of stimuli parameters

Now, we will study how the dominance times depend on the stimuli. The important stimulus characteristics are the intensity, modulation period p , bias

$b = |S_X|/|S_Y|$, and duty cycle d . Evidently, if we bias the system towards the state X by stimulating this neuron stronger than Y , i.e. $|S_X| > |S_Y|$, then the X neuron excitation period will dominate over the Y neuron excitation period. At the same time, the dominance depends on both the bias and the duty cycle.

The effect of the stimulus duty cycle d on the state dominance is illustrated in Fig. 11, where we plot the mean difference ($X - Y$) over the entire stimulation time for various bias levels b of the stimulus intensity. For $b > 1$, we observe the maximum in the X state dominance for $d \approx 0.5$ (50%). The decrease in the dominance for higher duty cycle ($d > 0.5$) reflects the effect of adaptation which is not strong enough for smaller d . Note that the extrema do not always occur at the 50% duty cycle because their location depends on the stimulus amplitude $|S_X|$.

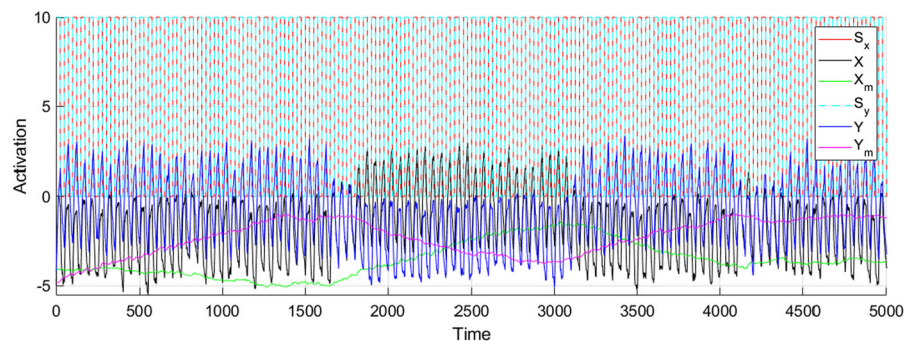
Similarly, the state Y dominates over the state X when the stimulus is biased towards Y ($b < 1$). For the unbiased stimulus ($b = 1$) case, the dominance is independent of the duty cycle and therefore averages to zero.

4.3.2 Effect of noise

The effect of noise on average dominance of the biased state depends on the duty cycle and bias values. The influence of noise on the dominance is illustrated in Fig. 12a, b for duty cycles $d = 0.5$ and $d = 1$, respectively. Interestingly, the dominance behavior in these graphs is completely different. While in the former case the absolute difference between X and Y tends to decrease with increasing noise intensity, for the latter case this value gradually grows.

The difference in the dominance behavior in Fig. 12a, b can be understood from the following

Fig. 10 Neuron activation under square-shape stimulation for $\eta = 0.1$



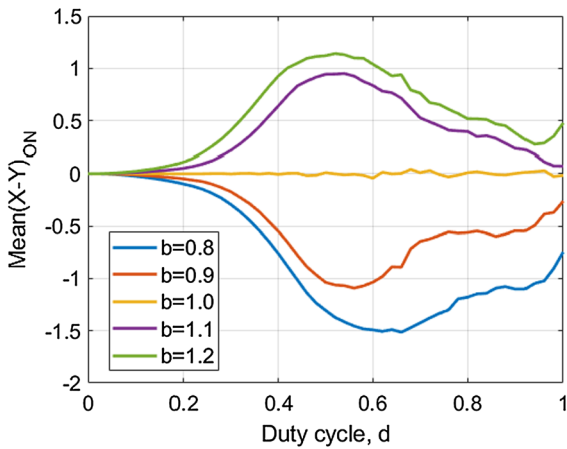
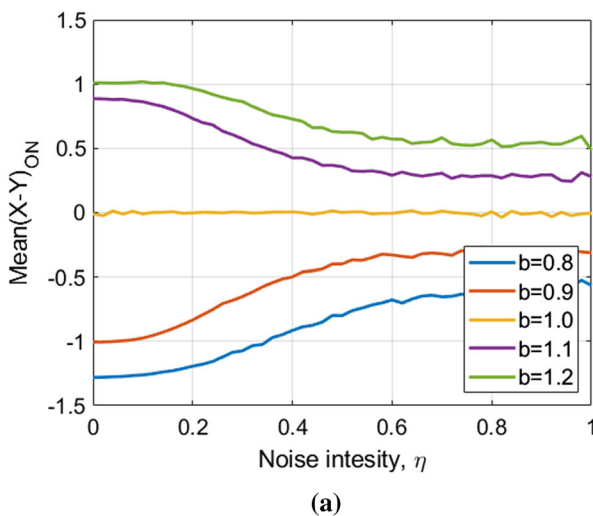


Fig. 11 Dominance of state X over state Y as a function of stimulus duty cycle d for various bias levels b and $\eta = 0.1$

consideration. In our model we suppose that the memory time scale is much larger than the perception time. Moreover, the memory of each perception state acts as a driving force behind adaptation. Adding highly erratic perturbations to the perceptual state causes the heavily inertial memory to evolve and adapt even slower. One can think of it in the sense that we do not retain a particular piece of information until we are certain about its perception, and not when the perception itself changes erratically. This way, noise suppresses adaptation and enables biased stimulation to increase the dominance of a chosen state, as can be seen in Fig. 12b. However, this does not mean that the increasing noise intensity for high duty cycles would



entail that the number of switches between the states decreases. On the contrary, with a 100% duty cycle, the number of switches between two states enlarges, as the noise intensity is increased (Fig. 6).

5 Discussion

Let us now discuss the most relevant outcomes of the proposed model and its adequacy for the description of experimental results.

5.1 Dominance duration distribution

We have shown that for certain values of the noise intensities the probability distribution of dominance durations is well approximated by gamma or log-normal distribution [29, 32]. As we already mentioned above, this type of distribution is typical for biological systems [29, 38]. Moreover, the mode dominance duration evaluated from the distributions decreases as the noise intensity is increased. This was confirmed by numerous psychological and neurophysiological experiments with bistable stimuli (see, e.g., [38, 43]), where more frequent switches between coexisting percepts were detected in subjects with stronger brain noise. Recent experimental studies [7] have shown that dominance times decreases linearly with noise, as the graph in Fig. 8 displays in the vicinity $\eta = 0.3$. Therefore, our model quantitatively

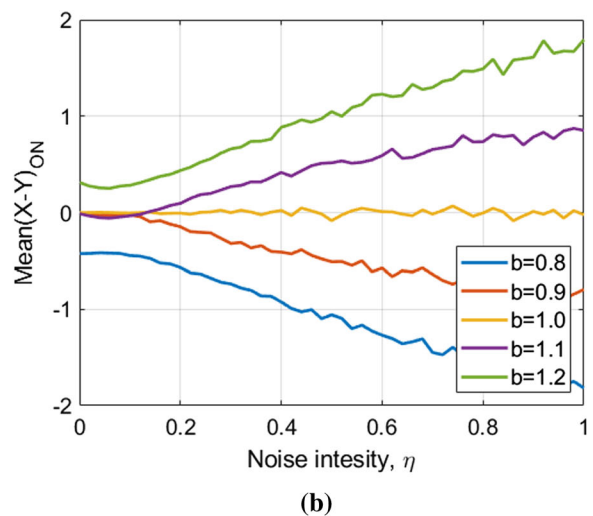


Fig. 12 Dominance versus noise intensity for various bias levels for **a** 50% and **b** 100% stimulus duty cycle

matches the actual experiments on humans when we choose the noise intensity to be around $\eta = 0.3$.

5.2 Implementation of adaptation with noise

Although our model is similar to that proposed by Huguet et al. [21], the two models yield fundamentally different results concerning the relative adaptation and noise intensities. While in the Huguet's model, the effect of adaptation is weaker than the noise effect and insufficient to induce switches between the states, in our model the adaptation is strong enough to cause switches even in the absence of noise, though with a higher effort.

In the psychological experiments with the bistable Necker cube [43], switches between two different percepts were studied under a time-varying control parameter and compared with a generic double-potential energy model. Recently, Meilikhov et al. [37] reported that in these experiments only brain noise is not able to induce jumps between two perceptual states, and therefore a change in the control parameter is needed. They found that brain noise only provided 15–40% of the energy gap among the subjects who participated in the discussed experiment [43]. This further validates our model showing that the adaptation effect prevails over the noise effect.

Another model that can be considered similar, but different in terms of synaptic connection is the *generalized firing rate model* proposed in the book of Ermentrout and Terman [11]. Their approach implies first summarizing all synaptic inputs before passing them through a sigmoidal function, $\sigma(X)$, like in our model, but with $\beta = 1$. Differing from the generalized firing rate model, we pass each synaptic input separately through $\sigma(X)$ and then add them to determine dynamics of each perceptual state. The previous approach implies that only a single neuron represents each state while a synaptic input from all synapses first enters the cell body and then it is collectively processed and passes forward through the axon. Instead, as indicated above, we consider a cluster of neurons, whose collective activity represents a perceptual state. In this cluster, the neurons are not connected all-to-all, but only to a specialized group of cells, such as corresponding memory cells or parallel activation cells of another perceptual state. The total cluster activity is the result of superposition of the activity of all the neuron sub-populations within the

cluster. Another minor difference of our model from the previous one is that our model carefully refrains from committing the perceptual activation variable with either membrane potential or spiking rate of the neurons. This allows us to generalize our approach to both domains by keeping the same dynamical characteristics.

It is important to realize that there are about 86 billion neurons in the human brain [18] and thus something of the same order in the visual cortex. In our model, we superpose the activity of all neurons representing a feature in each hemisphere and neglect the spatial variation across the surface. In spite of the crude approximation, our model is adequate for qualitative simulation of some neurophysiological experiments. For instance, the most popular neuroimaging modality, EEG, often records neuronal activity in the visual cortex from two hemispheres by using only two channels (O_1 and O_2) in the most basic setups. Other techniques, such as MEG and functional magnetic resonance imaging (fMRI) also do not have very high spatial resolution.

5.3 Perception stabilization effect

As discussed above, perceptual alternation can be brought to a standstill, if a visual stimulus is periodically removed from view (habituation). In the context of our model, this would be the case when the stimulus duty cycle is low enough to avoid adaptation effects (0–50% duty) as demonstrated in Sect. 4.3.

Recently, Dotov et al. [10] argue that the internal brain dynamics is inherently unstable due to adaptation forces, but with cues from the experience acting as contextual constraints, the competition between the percepts increases. As a result, we are able to make stable perceptual decisions in our every day practice. On the contrary, stimuli selected for experiments are special and contextually impoverished.

Visual perception can be biased if one or more of object features, as represented in the visual cortex feature-space, are additionally stimulated. For example, the perceived rotation direction of an ambiguously rotating sphere concurring with hand rotation is biased in the direction of the hand rotation [36].

Another method to bias the perception is based on memory. A more frequently observed perception uses a neuronal network activated multiple times in the past. The repeated activation renders synapses more

conductive to the neuronal current. Naturally, the next stimulus more likely activates this network as compared to more resistive less frequent perception.

Lastly, let us discuss the significance of the obtained results for the average dominance time versus noise intensity in the case of a 100% duty cycle. The results imply that for a constantly biased stimulus, such as, e.g., a stationary Necker cube image which can be interpreted as either left- or right-oriented, when the contrast of the inner lines giving preference for the left orientation is higher, when viewed for a prolonged time is perceived as a left-oriented cube more often than a right-oriented cube during the entire experiment duration in subjects having stronger brain noise [41, 45].

5.4 Biological relevance

Since the brain structure is symmetric, having two hemispheres including the visual cortex, we conjecture that every brain tends to have feature-specific neuronal clusters composed of two sub-populations, representing extreme ends of those features that constantly compete with each other to process the observed object.

Popularly, this dynamical process is treated using the metaphor of a ball traveling along an energy landscape assisted by “noisy” pushes [15]. For an ambiguous image, the two extremes can be visualized as energy wells with the same characteristic depth. However, for a biased stimulus, such as a completely left-oriented Necker cube, the corresponding energy well is so deep due to perceptual learning of this orientation, that it cannot be overcome by adaptation or noise.

Another paradigmatic example of a bistable stimulus is a “blue-and-black dress”, which is unique in the sense that its perception does not switch for most subjects (Fig. 13). This image, recently popularized in social media, was found to have two main perceptual states. In the interesting study of Lafer-Sousa et al. [26] with 1400 respondents, 57% persons saw the dress blue and black, 30% white and gold, 11% blue and brown, and 10% could switch between two different colors, while the remaining respondents perceived it as blue and gold. The dress was disproportionately seen as white and gold by women and elders. In addition, if we balance the illumination of seeing the picture, the dress becomes ambiguous and



Fig. 13 The blue-and-black dress image

highly bistable. The authors conclude that since the illumination is different for each individual due to perceptual learning, it produces a strong bias affect for each person.

Perception as a whole is composed of both adaptation and noise at its core. Adaptation provides the inherent tendency of brain to eventually switch between the two perceptual states by destabilizing the current state. This deterministic mechanism is crucial for switching between alternated perceptual decisions of comparable energy-well depths and avoid settling for the first deep decision one may come across. At the same time, the stochastic mechanism allows the system to effortlessly traverse through the energy landscape avoiding shallow energy wells that can be overcome solely by noise.

6 Conclusion

In this paper, we have developed a biologically relevant stochastic perception model based on adaptation, and carried out analytical and numerical analyses of this model. The comparison of the results of numerical simulations with recent neurophysiological experiments allowed us to conclude that our model, with adequate parameters, can be successfully used for a qualitative description of biological experiments, in particular, gamma distribution of dominance times and their decrease with increasing noise intensity.

Acknowledgements A.N.P. thanks the Spanish Ministry of Economy and Competitiveness for supporting the idea of this research under project SAF2016-80240. The data analysis was supported by the Russian Science Foundation (Grant No. 19-12-00050). The authors thank Dr. Gregor Schöner for fruitful discussions on setting up the initial model.

Compliance with ethical standards

Conflict of interest The authors declare that they have no conflict of interest.

References

- Blake, R., Logothetis, N.K.: Visual competition. *Nat. Rev. Neurosci.* **3**, 13–21 (2002)
- Boccaletti, S., Pisarchik, A.N., del Genio, C.I., Amann, A.: *From Coupled Systems to Complex Networks*. Cambridge University Press, Cambridge (2018)
- Brascamp, J.W., van Ee, R., Noest, A.J., Jacobs, R.H.A.H., van den Berg, A.V.: The time course of binocular rivalry reveals a fundamental role of noise. *J. Vis.* **6**(11), 8 (2006). <https://doi.org/10.1167/6.11.8>
- Braun, J., Mattia, M.: Attractors and noise: twin drivers of decisions and multistability. *NeuroImage* **52**(3), 740–751 (2010). <https://doi.org/10.1016/j.neuroimage.2009.12.126>
- Burns, B.D.: *The Uncertain Nervous System*. Edward Arnold, London (1968)
- Carter, O.L., Pettigrew, J.D.: A common oscillator for perceptual rivalries? *Perception* **32**(3), 295–305 (2003). <https://doi.org/10.1068/p3472>
- Chholak, P., Maksimenko, V.A., Hramov, A.E., Pisarchik, A.N.: Estimating voluntary and involuntary attention in bistable visual perception: A MEG study. *bioRxiv* p. 2020.02.18.953653 (2020). doi: <https://doi.org/10.1101/2020.02.18.953653>
- Deco, G., Rolls, E.T., Romo, R.: Stochastic dynamics as a principle of brain function. *Progr. Neurobiol.* **88**(1), 1–16 (2009)
- d’Onofrio, A. (ed.): *Bounded Noises in Physics, Biology, and Engineering*. Springer, New York (2013)
- Dotov, D.G., Turvey, M.T., Frank, T.D.: Embodied gestalts: Unstable visual phenomena become stable when they are stimuli for competitive action selection. *Atten. Percept. Psychophys.* (2019). <https://doi.org/10.3758/s13414-019-01868-4>
- Ermentrout, B., Terman, D.H.: *Mathematical Foundations of Neuroscience*. Springer, Berlin (2010)
- García-Vellisca, M.A., Pisarchik, A.N., Jaimes-Reátegui, R.: Experimental evidence of deterministic coherence resonance in coupled chaotic systems with frequency mismatch. *Phys. Rev. E* **94**, 012218 (2016)
- Gayet, S., Paffen, C.L.E., Van der Stigchel, S.: Information matching the content of visual working memory is prioritized for conscious access. *Psychol. Sci.* **24**(12), 2472–80 (2013). <https://doi.org/10.1177/0956797613495882>
- Gilden, D.L., Thornton, T., Mallon, M.W.: 1/f noise in human cognition. *Science* **267**, 1837–1839 (1995)
- Haken, H.: *Principles of Brain Functioning*. Springer, Berlin (1996)
- Hausdorff, J.M., Peng, C.K.: Multiscaled randomness: a possible source of 1/f noise in biology. *Phys. Rev. E* **54**(2), 2154–2157 (1996)
- Hebb, D.O.: *The Organization of Behaviour*. Wiley, New York (1949)
- Herculano-Houzel, S.: The human brain in numbers: a linearly scaled-up primate brain. *Front. Hum. Neurosci.* **3**(Nov), 31 (2009). <https://doi.org/10.3389/neuro.09.031.2009>
- Hock, H.S., Schöner, G., Giese, M.: The dynamical foundations of motion pattern formation: stability, selective adaptation, and perceptual continuity. *Percept. Psychophys.* **65**(3), 429–457 (2003). <https://doi.org/10.3758/BF03194574>
- Hramov, A.E., Maksimenko, V.A., Koronovskii, A.A., Runnova, A.E., Zhuravlev, M.O., Pisarchik, A.N., Kurths, J.: Percept-related EEG classification using machine learning approach and features of functional brain connectivity. *Chaos* **29**, 093110 (2019)
- Huguet, G., Rinzel, J., Hupe, J.M.: Noise and adaptation in multistable perception: noise drives when to switch, adaptation determines percept choice. *J. Vis.* **14**(3), 19 (2014). <https://doi.org/10.1167/14.3.19>
- Jacobson, G.A., Diba, K., Yaron-Jakoubovitch, A., Oz, Y., Koch, C., Segev, I., Yarom, Y.: Subthreshold voltage noise of rat neocortical pyramidal neurons. *J. Physiol.* **564**(1), 145–160 (2005)
- Kelso, J.A.S.: Multistability and metastability: understanding dynamic coordination in the brain. *Philos. Trans. R. Soc. B* **32–33**(1591), 906–918 (2012). <https://doi.org/10.1098/rstb.2011.0351>
- Kohler, W., Wallach, H.: Figural after-effects, an investigation of visual processes. *Proc. Am. Philos. Soc.* **88**, 269–357 (1944)
- Kornmeier, J., Ehn, W., Bigalke, H., Bach, M.: Discontinuous presentation of ambiguous figures: how interstimulus interval durations affect reversal dynamics and ERPs. *Psychophysiology* **44**(4), 552–560 (2007)
- Lafer-Sousa, R., Hermann, K.L., Conway, B.R.: Striking individual differences in color perception uncovered by ‘the dress’ photograph. *Curr. Biol.* **25**(13), R545–R546 (2015). <https://doi.org/10.1016/J.CUB.2015.04.053>
- Lago-Fernández, L.F., Deco, G.: A model of binocular rivalry based on competition in IT. *Neurocomputing* **44–46**, 503–507 (2002). [https://doi.org/10.1016/S0925-2312\(02\)00408-3](https://doi.org/10.1016/S0925-2312(02)00408-3)
- Laing, C.R., Chow, C.C.: A spiking neuron model based for binocular rivalry. *J. Comput. Neurosci.* **12**, 39–53 (2002)
- Lehky, S.R.: An astable multivibrator model of binocular rivalry. *Perception* **17**(1988), 215–228 (1995)
- Leopold, D.A., Logothetis, N.K.: Multistable phenomena: changing views in perception. *Trends Cognit. Sci.* **3**(Regular), 254–264 (1999)
- Leopold, D.A., Wilke, M., Maier, A., Logothetis, N.K.: Stable perception of visually ambiguous patterns. *Nat. Neurosci.* **5**(6), 605–609 (2002). <https://doi.org/10.1038/nn0602-851>
- Levelt, W.J.M.: *On Binocular Rivalry*. Mouton, Paris (1968)

33. Long, G.M., Toppino, T.C.: Enduring interest in perceptual ambiguity: Alternating views of reversible figures. *Psychol. Bull.* **130**, 748–768 (2004)
34. Maksimenko, V.A., Frolov, N.S., Hramov, A.E., Runnova, A.E., Grubov, V.V., Kurths, J., Pisarchik, A.N.: Neural interactions in a spatially-distributed cortical network during attentional tasks. *Front. Behav. Neurosci.* **13**, 20 (2019)
35. Maksimenko, V.A., Hramov, A.E., Grubov, V.V., Nedaivozov, V.O., Makarov, V.V., Pisarchik, A.N.: Non-linear effect of biological feedback on brain attentional state. *Nonlinear Dyn.* **95**, 1923–1939 (2019)
36. Maruya, K., Yang, E., Blake, R.: Voluntary action influences visual competition. *Psychol. Sci.* **18**(12), 1090–1098 (2007). <https://doi.org/10.1111/j.1467-9280.2007.02030.x>
37. Meilikhov, E.Z., Farzetdinova, R.M.: Bistable perception of ambiguous images: simple Arrhenius model. *Cognit. Neurodyn.* (2019). <https://doi.org/10.1007/s11571-019-09554-9>
38. Merk, I., Schnakenberg, J.: A stochastic model of multistable visual perception. *Biol. Cyber.* **86**, 111–116 (2002)
39. Moreno-Bote, R., Rinzel, J., Rubin, N.: Noise-induced alternations in an attractor network model of perceptual bistability. *J. Neurophysiol.* **98**(3), 1125–39 (2007). <https://doi.org/10.1152/jn.001116.2007>
40. Pikovsky, A.S., Kurths, J.: Neural interactions in a spatially-distributed cortical network during attentional tasks. *Phys. Rev. Lett.* **13**, 78 (2019)
41. Pisarchik, A.N., Chholak, P., Hramov, A.E.: Brain noise estimation from MEG response to flickering visual stimulation. *Chaos Soliton. Fract. X* **1**, 100005 (2019). <https://doi.org/10.1016/J.CSFX.2019.100005>
42. Pisarchik, A.N., Jaimes-Reátegui, R.: Deterministic coherence resonance in coupled chaotic oscillators with frequency mismatch. *Phys. Rev. E* **92**, 050901(R) (2015)
43. Pisarchik, A.N., Jaimes-Reátegui, R., Magallón-García, C.D.A., Castillo-Morales, C.O.: Critical slowing down and noise-induced intermittency in bistable perception: bifurcation analysis. *Biol. Cybernet.* **108**(4), 397–404 (2014). <https://doi.org/10.1007/s00422-014-0607-5>
44. Quian Quiroga, R., Reddy, L., Kreiman, G., Koch, C., Fried, I.: Invariant visual representation by single neurons in the human brain. *Nature* **435**, 1102–1107 (2005). <https://doi.org/10.1038/nature03687DO>
45. Runnova, A.E., Hramov, A.E., Grubov, V.V., Koronovskii, A.A., Kurovskaya, M.K., Pisarchik, A.N.: Theoretical background and experimental measurements of human brain noise intensity in perception of ambiguous images. *Chaos Soliton Fract.* **93**, 201–206 (2016). <https://doi.org/10.1016/J.CHAOS.2016.11.001>
46. Scocchia, L., Valsecchi, M., Gegenfurtner, K.R., Triesch, J.: Differential effects of visual attention and working memory on binocular rivalry. *J. Vis.* (2014). <https://doi.org/10.1167/14.5.13>
47. Shpiro, A., Moreno-Bote, R., Rubin, N., Rinzel, J.: Balance between noise and adaptation in competition models of perceptual bistability. *J. Comput. Neurosci.* **27**(1), 37–54 (2009). <https://doi.org/10.1007/s10827-008-0125-3>
48. Sterzer, P., Kleinschmidt, A., Rees, G.: The neural bases of multistable perception. *Trends Cognit. Sci.* **13**(7), 310–318 (2009). <https://doi.org/10.1016/J.TICS.2009.04.006>
49. Urakawa, T., Bunya, M., Araki, O.: Involvement of the visual change detection process in facilitating perceptual alternation in the bistable image. *Cognit. Neurodyn.* **11**(4), 307–318 (2019)
50. Valdez, A.B., Papesh, M.H., Treiman, D.M., Smith, K.A., Goldinger, S.D., Steinmetz, P.N.: Distributed representation of visual objects by single neurons in the human brain. *J. Neurosci.* **35**(13), 5180–5186 (2015). <https://doi.org/10.1523/JNEUROSCI.1958-14.2015>
51. Wertheimer, M.: Experimentelle Studien über das Sehen von Bewegung. *Zeitschrift für Psychologie* **61**, 161–265 (1912)
52. Wilson, H.R., Blake, R., Lee, S.H.: Dynamics of travelling waves in visual perception. *Nature* **412**(6850), 907–910 (2001)

Publisher's Note Springer Nature remains neutral with regard to jurisdictional claims in published maps and institutional affiliations.